AMERICAN ACADEMY OF OPHTHALMOLOGY®

Distribution of OCT Features within Areas of Macular Atrophy or Scar after 2 Years of Anti-VEGF Treatment for Neovascular AMD in CATT

*Cynthia A. Toth, MD,[1,2] Vincent Tai, MS,[1] Maxwell Pistilli, MS,[3] Stephanie J. Chiu, PhD,[1] Katrina P. Winter, BS,[1] Ebenezer Daniel, MBBS, PhD,[3] Juan E. Grunwald, MD,[3] Glenn J. Jaffe, MD,[1] Daniel F. Martin, MD,[4] Gui-shuang Ying, PhD,[2] Sina Farsiu, PhD,[2] Maureen G. Maguire, PhD,[3] for the Comparison of Age-related Macular Degeneration Treatments Trials Research Group**

Purpose: Macular atrophy and scar increase in prevalence during treatment for neovascular age-related macular degeneration and are associated with poor visual acuity. We sought to identify the distribution of spectral-domain OCT (SD-OCT)-determined features and subretinal lesion thicknesses at sites of macular scar or atrophy after 2 years of treatment in the Comparison of Age-Related Macular Degeneration Treatments Trials (CATT).

Design: Cross-sectional analysis.

Participants: CATT participants with SD-OCT, color photographic (CP) and fluorescein angiogram (FA; CP/FA) images at year 2.

Methods: Sixty-eight study eyes at year 2 in CATT were selected based on image quality and CP/FA-determined predominant presence of the following: geographic atrophy (GA, n = 25), non-GA (NGA, n = 44), fibrotic scar (FS, n = 26), or non-FS (NFS, n = 7). The CP/FA components were delineated by CP/FA readers; SD-OCT morphologic features and thicknesses were delineated by OCT readers. Using custom software and graphic user interfaces, images were registered, overlaying features and components per pixel; differences were analyzed across groups.

Main Outcome Measures: OCT features, CP/FA components, and retinal and subretinal lesion thicknesses at each pixel of regional overlays.

Results: SD-OCT assessment of registered areas of pathology revealed the following: (1) retinal pigment epithelium atrophy (with or without residual lesion material) covered 75% of pixels designated as GA, 22% of NGA, 24% of NFS, and 46% of FS ($P < 0.001$). (2) Photoreceptor layer thinning covered 85% of GA, 42% of NGA, 33% of NFS, and 59% of FS ($P < 0.001$). (3) Subretinal lesion features covered 31% of GA, 42% of NGA, 85% of NFS, and 92% of FS ($P < 0.001$). Mean thickness of the subretinal lesion complex (measured in microns ± standard deviation) differed among GA (48±25 μm), NGA (61±35 μm), NFS (83±17 μm), and FS (151±74 μm) ($P < 0.001$). In eyes with GA, the thickness was greater in areas with residual lesion (51.4±27 μm) than in those without (27.2±9 μm).

Conclusions: Retinal pigment epithelium atrophy and photoreceptor layer thinning are common not only in areas of macular atrophy but also in areas of FS. Photoreceptor loss extends beyond the areas of clinically apparent atrophy and FS. Subretinal lesion components were common in areas of scar, but they were also present in nearly one-third or more of areas of macular atrophy. *Ophthalmology Retina 2019;3:316-325 © 2018 by the American Academy of Ophthalmology*

Supplemental material available at www.ophthalmologyretina.org.

Despite early recovery of visual acuity (VA) with anti−vascular endothelial growth factor (VEGF) treatment in the majority of eyes with active subfoveal neovascular age-related macular degeneration (nAMD), VA in these eyes typically declines over subsequent years of treatment. We lack a clear understanding of the complex interrelated microanatomic changes in nAMD, their evolution during anti-VEGF treatment, and their relationship to concurrent and future VA. These relationships have been studied in nAMD through analysis of retinal images, most commonly color photographs (CP), fluorescein angiograms (FA), and OCT. Many of the analyses correlating the findings across imaging modalities have centered on the presence and location of fluid surrounding the neovascularization,

https://doi.org/10.1016/j.oret.2018.11.011
ISSN 2468-6530/19

particularly on areas of fluid leakage designated as intraretinal fluid (IRF), subretinal fluid (SRF), and subretinal pigment epithelial (sub-RPE) fluid on OCT imaging.

Both geographic atrophy (GA) and scar are more prevalent at 2 years after the start of anti-VEGF treatment than at baseline,[1-5] and the presence of each of these pathologic features is associated with poorer VA.[6,7] However, on CP and FA, it is not possible to distinguish the retinal and subretinal components of these late-stage lesions.

There is a robust body of evidence to demonstrate the relationship between fluid location on OCT images in nAMD and VA before and after anti-VEGF treatment[6,8,9] and to link atrophy and scar to VA loss during anti-VEGF treatment.[4,7,10-12] However, analyses that assess the relation of OCT features to specific regions of macular atrophy, GA, or scar based on CP/FA after anti-VEGF treatment are lacking. We hypothesized that if we could accurately and precisely correlate information from CP/FA and OCT at a specific pathology site, that we would identify common retinal and subretinal anatomic elements that would help to explain VA loss, thus identifying a potential pharmacologic target that might help preserve VA in nAMD. Optical coherence tomography imaging of the retinal and subretinal findings at the site of fibrosis or atrophy could also clarify disparate and common pathways of morphology change, leading to greater understanding of the pathophysiology of the lesion response at 2 years. Therefore, in this study we analyzed data from eyes with areas designated on CP/FA as GA, nongeographic atrophy (NGA), fibrous scar (FS), or nonfibrous scar (NFS) in the macula at the 2-year visit in the Comparison of Age-Related Macular Degeneration Treatments Trials (CATT). To extract this information, we used previously published methods to register and assess OCT features within areas given the previous designations based on CP/FA.

Methods

The participants in and methods of CATT have been described in a previous publication[13] and at the ClinicalTrials.gov website (NCT00593450). Enrollment extended across 43 clinical centers in the United States from February 2008 to December 2009. The study was approved by an institutional review board associated with each center and was compliant with the Health Insurance Portability and Accountability Act regulations. The study was performed in accordance with the tenets of the Declaration of Helsinki. All participants provided written informed consent.

The image analysis methods have been published previously.[13] Briefly, the CATT participants had bilateral stereo CP, stereo FA, and time-domain OCT (TD-OCT) at baseline. Color photographs, FA, and OCT were repeated at 1, 2, and 5 years, and SD-OCT was captured in many of the CATT participants after the year 1 visit. Thus, year 2 (104-week visit) scans were either captured with TD-OCT or SD-OCT. Only SD-OCT scans were used in this study because of their denser pattern of capture and higher resolution than TD-OCT. The SD-OCT systems included Cirrus (Carl Zeiss Meditec, Dublin, CA) and Spectralis (Heidelberg Engineering, Heidelberg Germany), with scan patterns as previously reported.[13] Photographic images were evaluated by the CATT Fundus Photograph Reading Center (University of Pennsylvania, Philadelphia, PA), and OCT images were evaluated by certified readers at the CATT OCT Reading Center (Duke University, Durham, NC). The location of specific SD-OCT features was delineated by readers at Dr. Toth's Duke Advanced Research in Swept Source/SD-OCT Imaging Laboratory (Duke University). Readers at each reading center were masked to the assessment from the other reading center.[13]

Four main features identifiable on stereo CP/FA images of eyes treated with anti-VEGF agents were selected for in-depth evaluation based on the prior Photograph Reading Center definitions: (1) GA, (2) NGA, (3) FS, and (4) NFS[13] (definitions in Table 1). Although we recognize the controversy over the use of the term "geographic area" for macular atrophy after nAMD treatment, we retained the GA terminology because our original categorization of atrophic findings into two mutually exclusive lesion components, GA or NGA, used this language. The CATT Coordinating Center selected 70 eyes of 70 participants at the 104-week CATT visit with one or more of these features present on CP/FA and with SD-OCT scans using stratified sampling to obtain a representative sample of images with these features present at the fovea or outside the fovea. Because of the complexity of the overlay analyses, we did not include nAMD lesions without at least one of these components. It was not possible to analyze photographic or OCT images on 2 of the 70 eyes because of inadequate image quality.

To analyze photographs, CP/FA lesion components were marked within a 6-mm circular region centered on the fovea. To analyze SD-OCT images, retinal and subretinal features were marked, and retinal and subretinal boundaries were segmented to determine lesion thicknesses across the SD-OCT volume scans. These markings and the methods for image overlay are detailed by Toth et al[13] and summarized later.

For CP/FA images, graders delineated the total choroidal neovascularization (CNV) lesion (TCNVL) and 10 component morphologic features as previously described[13] (Fig 1): CNV, hemorrhage, FS, NFS, serous pigment epithelial detachment (PED), blocked fluorescence, GA, NGA, retinal angiomatous proliferation, and RPE tear. Each morphology was outlined with a unique color, and each of the 10 components was exclusive at any single location so that a site could not be assigned more than one component. In addition to lesion components, we designated "nonlesion" regions as CP/FA or OCT areas without marked lesion components.

For SD-OCT, readers used proprietary software, Duke OCT Retinal Analysis Program (DOCTRAP) Marking Code Version 61.4.2 developed in MATLAB R2012a (MathWorks, Natick, MA) to mark the foveal center, optic disc center, and the lateral extent of 11 morphologic features within every B-scan of the macular volumes as previously described (see Fig 1): intraretinal fluid (IRF), outer retinal tubulation (ORT; hyperreflective rosettes, similar to and thought to reflect early development of ORT, although marked separately, were combined within the category ORT for this analysis), SRF, subretinal highly reflective material (SHRM), nondrusenoid PED, indeterminate SHRM/PED, sub-RPE fluid, and photoreceptor layer thinning. We also marked RPE atrophy with choroidal hypertransmission (called RPE atrophy), which could be present with or without overlying lesion material. Although most SD-OCT features could be colocalized at the same pixel location (e.g., IRF, SHRM, and PED), by definition, RPE atrophy without overlying lesion was mutually exclusive with all of the following: SHRM, PED, indistinguishable SHRM/PED, sub-RPE fluid, and RPE atrophy with overlying lesion material. Thickness of the RPE + drusen + lesion complex (RPEDLC, RPE plus all drusen material, whether above or below the RPE, plus all subretinal/sub-RPE lesion components plus subretinal/sub-RPE fluid) was extracted from

Table 1. Frequency and Median of the Percentage of Pixels of OCT Features within Each Color Photographic/Fluorescein Angiographic Component of 68 Study Eyes

		CP/FA component					No CP/FA Component
		Geographic Atrophy (n = 25)	Nongeographic Atrophy (n = 44)	Nonfibrotic Scar (n = 7)	Fibrotic Scar (n = 26)		Macular Area Outside Total CNV lesion (n = 68)
	Eyes containing any pixels of OCT feature	n (%)	n (%)	n (%)	n (%)		**n (%)**
OCT feature	**Percent of pixels with OCT features within the CP/FA component***	Median (25%, 75%)	Median (25%, 75%)	Median (25%, 75%)	Median (25%, 75%)	***P***	**Median (25%, 75%)**
RPE atrophy with choroidal hypertransmission	Eyes	25 (100)	42 (95)	4 (57)	23 (88)	0.005	58 (85)
	% Pixels	75 (66, 86)	22 (7, 44)	24 (18, 49)	46 (24, 64)	<0.001	3 (1, 10)
RPE atrophy without overlying lesion	Eyes	20 (80)	14 (32)	0 (0)	4 (15)	<0.001	20 (29)
	% Pixels	25 (12, 39)	1 (0, 2)	N/A	2 (0, 5)	<0.001	1 (0, 3)
RPE atrophy with overlying lesion	Eyes	25 (100)	42 (95)	4 (57)	23 (88)	0.005	58 (85)
	% Pixels	52 (38, 62)	22 (7, 43)	24 (18, 49)	46 (24, 64)	<0.001	3 (1, 7)
Photoreceptor loss	Eyes	25 (100)	42 (95)	4 (57)	23 (88)	0.005	65 (96)
	% Pixels	85 (66, 92)	42 (22, 61)	33 (22, 67)	59 (33, 78)	<0.001	7 (3, 19)
Outer retinal tubulation	Eyes	9 (36)	21 (48)	1 (14)	11 (42)	0.40	15 (22)
	% Pixels	1 (0, 2)	1 (0, 3)	4 (4, 4)	1 (1, 8)	0.49	0 (0, 0)
Subretinal lesion	Eyes	20 (80)	42 (95)	7 (100)	26 (100)	0.04	65 (96)
	% Pixels	31 (13, 69)	42 (19, 66)	85 (64, 95)	92 (88, 100)	<0.001	3 (1, 6)
SHRM	Eyes	14 (56)	28 (64)	4 (57)	22 (85)	0.11	37 (54)
	% Pixels	27 (3, 40)	8 (2, 25)	16 (14, 33)	71 (47, 81)	<0.001	0 (0, 1)
PED	Eyes	19 (76)	42 (95)	7 (100)	26 (100)	0.01	64 (94)
	% Pixels	18 (9, 52)	32 (16, 66)	72 (49, 95)	80 (47, 95)	<0.001	3 (1, 6)
Indeterminate SHRM/PED	Eyes	13 (52)	23 (52)	3 (43)	9 (35)	0.49	27 (40)
	% Pixels	3 (1, 8)	2 (1, 6)	9 (2, 12)	4 (3, 4)	0.66	0 (0, 0)
Any fluid	Eyes	16 (64)	26 (59)	3 (43)	19 (73)	0.44	41 (60)
	% Pixels	2 (0, 16)	3 (0, 23)	6 (2 25)	14 (1, 49)	0.45	1 (0, 2)
Intraretinal fluid	Eyes	16 (64)	23 (52)	2 (29)	16 (62)	0.36	36 (53)
	% Pixels	2 (0, 14)	1 (0, 3)	13 (1, 25)	4 (1, 18)	0.10	0 (0, 1)
Subretinal fluid	Eyes	4 (16)	14 (32)	2 (29)	8 (31)	0.51	20 (29)
	% Pixels	1 (0, 1)	9 (0, 30)	3 (1, 6)	4 (1, 43)	0.26	1 (0, 6)
Sub-RPE fluid	Eyes	3 (12)	8 (18)	0 (0)	4 (15)	0.82	6 (9)
	% Pixels	0 (0, 3)	1 (0, 10)	N/A	26 (6, 53)	0.26	0 (0, 0)
Absent the above OCT features	Eyes	23 (92)	43 (98)	4 (57)	18 (69)	<0.001	68 (100)
	% Pixels	6 (3, 12)	27 (12, 54)	20 (10, 27)	3 (1, 9)	<0.001	87 (74, 94)

CNV = choroidal neovascularization; CP = color photographs; FA = fluorescein angiograms; PED = pigment epithelial detachment; RPE = retinal pigment epithelium; SHRM = subretinal highly reflective material; subretinal lesion includes SHRM, PED, and indeterminate SHRM/PED.
One eye may have multiple CP/FA components.
*The percentage of pixels in the CP/FA component is only from those eyes that contained any of the respective OCT features. For example, in 42 eyes with nongeographic area, a median of 22% of pixels contained the OCT feature of RPE atrophy.

semiautomated segmentation of scans across a 5-mm diameter circular region centered on the fovea.[14] Thickness of the neurosensory retina (NSR, retina without subretinal lesion complex or RPE) was also measured across this region. Because of the variable thickness of the NSR across the fovea, the thickness was reported relative to the mean thickness at that foveal location, based on a dataset from 115 eyes of 119 control participants, mean age 67 years (range 51–83 years) without AMD from the Age-Related Eye Disease Study 2 ancillary SD-OCT study.[15]

Photographic and OCT overlay images were manually registered and pixels were interpolated. Color photographs/fluorescein angiograms and OCT markings were compared side by side, and overlays of the SD-OCT and CP/FA data were extracted pixel by pixel using custom MATLAB software with a graphic user interface (CATTREG V2.9, developed in the Duke Advanced Research in Swept Source/SD-OCT Imaging Laboratory by CAT, VT, and SJC) for a 5-mm diameter circular region. The software produced a dataset containing each pixel's location on a standardized grid, and for each pixel, a binary value for the presence of each OCT feature

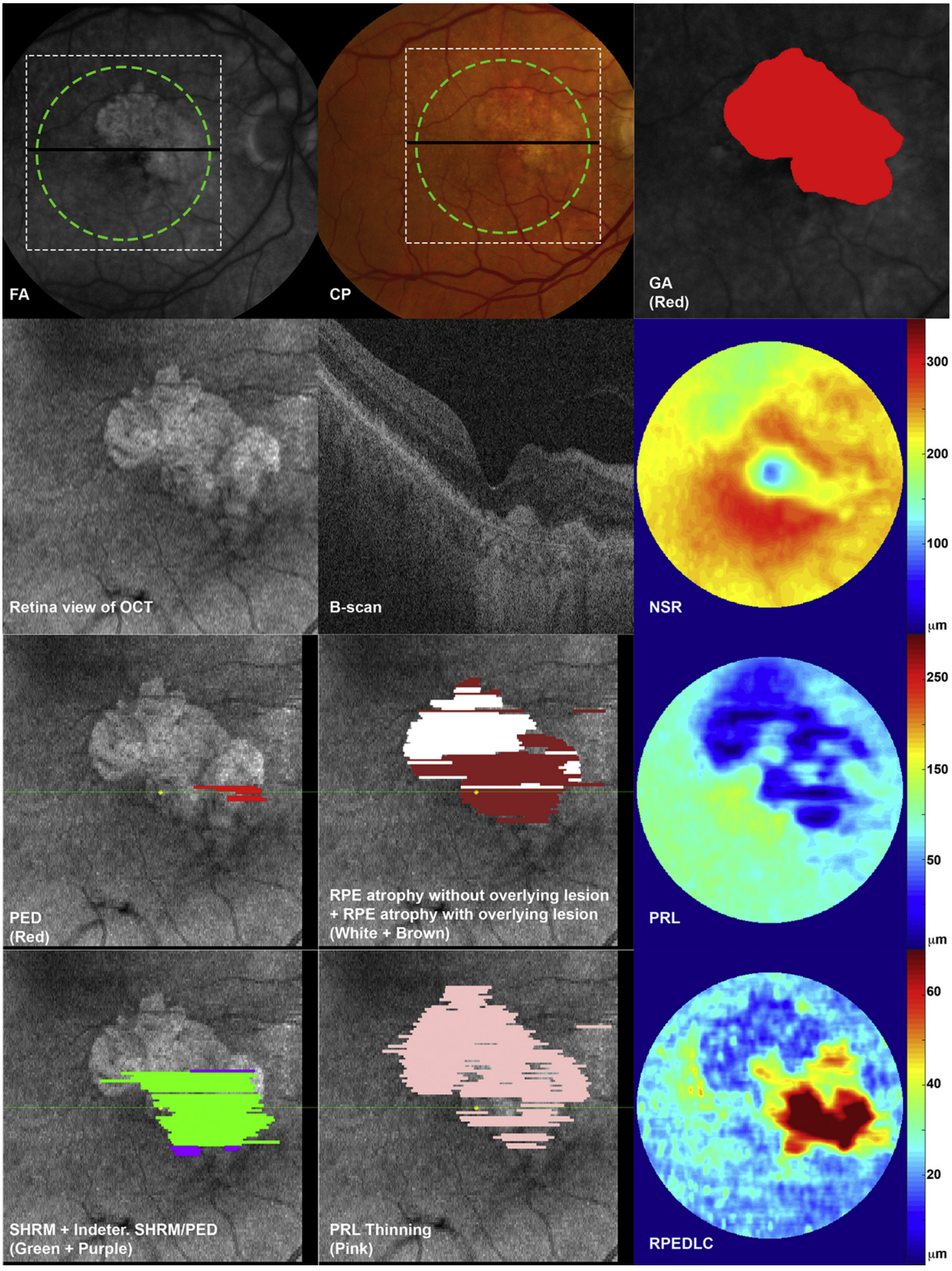

Figure 1. Overlay of color photographic/fluorescein angiographic (CP/FA)-designated characteristics and OCT-designated features and thicknesses on aligned macular regions at the year 2 visit in CATT for an eye with predominant CP/FA-designated geographic atrophy and predominant CP/FA-designated fibrotic scar. CATT = Comparison of Age-Related Macular Degeneration Treatments Trials; GA = geographic atrophy; NSR = neurosensory retina; PED = nondrusenoid pigment epithelial detachment; PRL = photoreceptor layer; RPE = retinal pigment epithelium; RPEDLC = RPE + drusen + lesion complex; SHRM = subretinal highly reflectively material.

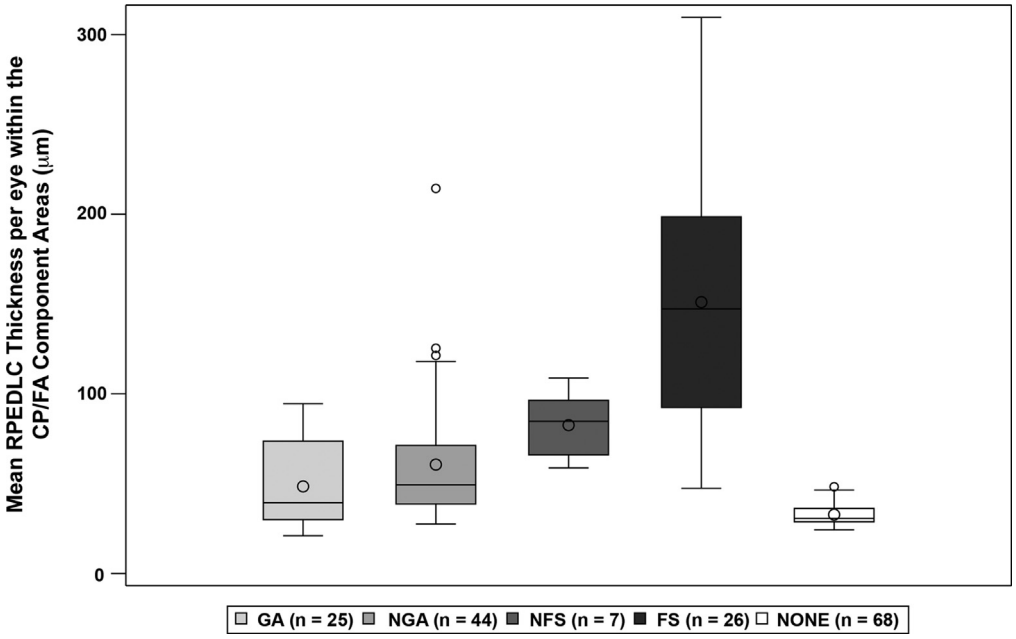

Figure 2. Distribution among eyes of the mean thickness on OCT of the RPEDLC for the pixels within each color photograph (CP)/fluorescein angiographic (FA) component. FS = fibrotic scar; GA = geographic atrophy; NFS = nonfibrotic scar; NGA = nongeographic atrophy; NONE = macular areas without any lesion components; RPEDLC = retinal pigment epithelium + drusen + lesion complex. Box-and-whisker plots: Box upper and lower edges correspond to the 75th and 25th percentiles, respectively. Within the box, the circle corresponds to the mean value and the line corresponds to the 50th percentile (median). Ends of whiskers correspond to the lowest score within 1.5 times the interquartile range of the 25th percentile and the highest score within 1.5 times the interquartile range of 75th percentile. Each circle outside the whiskers corresponds to outliers of the score.

or CP/FA component, and OCT thickness measurements. We analyzed the frequency of OCT features within the CP/FA components of each of the 68 study eyes. We also evaluated the percentage of pixels covered by OCT features within the total pixel area of each of the 4 distinct CP/FA lesion components and also the area outside the CP/FA TCNVL for each eye. To evaluate the relationship between layer thicknesses and qualitative SD-OCT morphology within the CP/FA components, we determined the NSR or RPEDLC thickness for the pixels of selected OCT features within the 4 CP/FA components.

Statistical Analysis

We used Fisher exact tests to compare the frequency of the OCT features within the CP/FA components in eyes. We also determined the median and quartiles of the percentage of pixels containing OCT features per designated CP/FA component area in each eye for which OCT data were available. We subsequently determined the percentage of each of the 4 CP/FA component pixels that was occupied by different OCT features alone and in combination. We compared the median values between CP/FA features using Kruskal–Wallis tests. We also calculated the mean thickness and volume of the RPEDLC for pixels designated as each of the 4 CP/FA features and for the nonfeature region and compared them using Kruskal–Wallis tests.

Results

Within the 68 eyes of 68 participants at the 104-week CATT visit, the 4 CP/FA lesion components were represented as follows: 25 eyes had GA, 44 eyes had NGA, 26 eyes had FS, and 7 eyes had NFS. More than one CP/FA lesion component was present in more than a third of the eyes. When present, GA, NGA, FS, and NFS constituted a median of 17%, 28%, 12%, and 2%, respectively, of the 5-mm diameter circular region area.

The frequency of OCT features within the CP/FA components and within the areas outside the CP/FA-designated total CNV lesion components is shown in Table 1 in the rows labeled "Eyes." The percentage of pixels covered by OCT features within the total pixel area of each of the 4 distinct CP/FA lesion components and within the areas outside the CP/FA total CNV lesion for each eye is shown in Table 1 in the rows labeled "% Pixels." The thicknesses of the RPEDLC and of the variance in NSR thickness relative to normative data for aged eyes are shown in Figures 2 and 3. These findings are addressed in detail later. A cross-tabulation between the different OCT features at the same pixel location is shown in Table S2 (available at http://www.ophthalmologyretina.org).

Optical coherence tomography features of RPE atrophy with choroidal hypertransmission included areas with and without residual lesion material. The majority of RPE atrophy without overlying lesion was found almost exclusively in GA: it was present in 80% of GA eyes and covered a median of 25% of GA pixels in those eyes. The next closest amount was in NGA, where it covered a median of 1% of pixels in 32% of NGA eyes; it was rarely found in NFS and was not present in eyes with FS (see Table 1). In contrast, RPE atrophy with overlying lesion was present in areas of atrophy and of scar; it was present in 100% of eyes with GA, 95% with NGA, 88% with FS, and 57% with NFS, respectively. Notably, it covered an additional median 52% of GA pixels, 22% of NGA pixels, 46% of FS pixels, and 24% of NFS pixels in eyes containing these components. Furthermore, within GA, the mean (± standard deviation) thickness of the RPEDLC was different between areas of RPE atrophy with overlying lesion (51.4±27 μm) versus RPE atrophy without

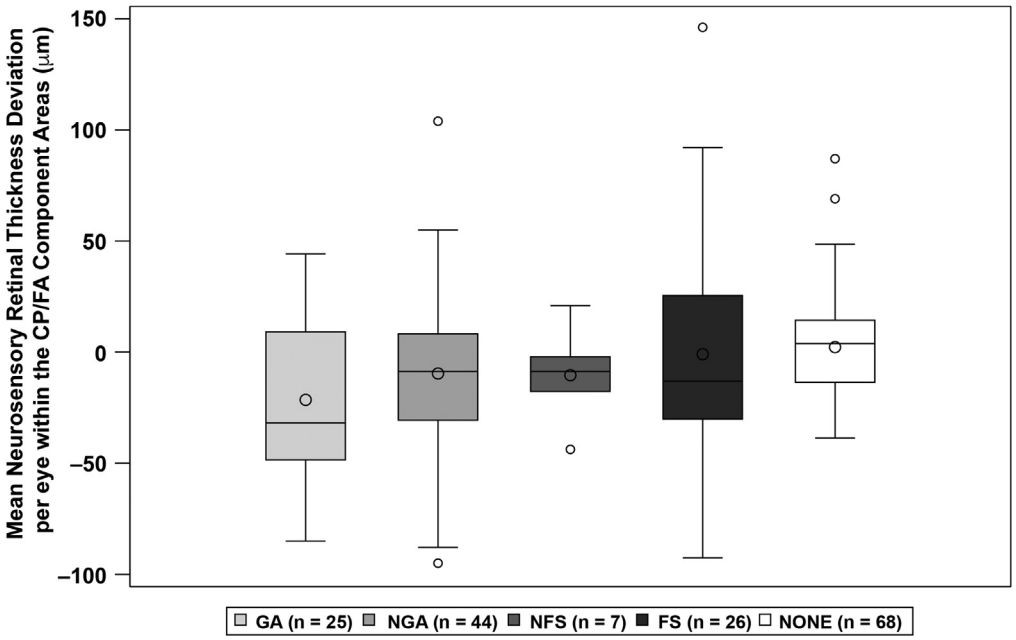

Figure 3. Distribution among eyes of the mean retinal thickness on OCT for the pixels within each color photograph (CP)/fluorescein angiographic (FA) component. FS = fibrotic scar, GA = geographic atrophy, NFS = nonfibrotic scar, NGA = nongeographic atrophy, and NONE = macular areas without any lesion components. Box-and-whisker plots: Box upper and lower edges correspond to the 75th and 25th percentiles, respectively. Within the box, the circle corresponds to the mean value and the line corresponds to the 50th percentile (median). Ends of whiskers correspond to the lowest score within 1.5 times the interquartile range of the 25th percentile and the highest score within 1.5 times the interquartile range of 75th percentile. Each circle outside the whiskers corresponds to outliers of the score.

overlying lesion (27.2±9 μm, $P < 0.001$). Within areas of FS, the mean thickness of the RPEDLC was not different between areas with and without RPE atrophy with choroidal hypertransmission (140±64 μm vs. 153±90 μm, $P = 0.23$), all of which had residual lesion present.

Photoreceptor layer thinning visible to the OCT reader extended over a median of 76% of pixels designated as RPE atrophy with choroidal hypertransmission; the photoreceptor loss covered a median of 95% of pixels over RPE atrophy without an overlying lesion and 73% over RPE atrophy with an overlying lesion. Although the frequency of photoreceptor loss matched that of the RPE atrophy, photoreceptor loss extended across a larger median percentage of pixels than did RPE atrophy for all lesion components: a median of 85% (photoreceptor loss) versus 75% (RPE atrophy) for the GA area, 42% versus 22% for the NGA area, 59% versus 46% for the FS area, and 33% versus 24% for the NFS scar area (see Table 1). The qualitative finding of photoreceptor loss by readers was not distinguished by deviation in NSR thickness relative to normative data for aged eyes except in those with GA. Across GA, mean NSR deviation relative to normal was −22±35 μm (Fig. 3). Outer retinal tubulations, thought to represent photoreceptor degeneration, were uncommon in NFS lesions (14%) and present in similar frequency in GA, NGA, and FS (36 to 48%), although they involved minimal lesion component area (medians were ≤4% of the area).

An OCT subretinal lesion feature (SHRM, PED, or indeterminate SHRM or PED) was present within the lesion component in 80% of eyes with GA, in 95% with NGA, and in 100% with NFS and FS and involved a median of 31% of the GA area, 42% of the NGA area, 85% of the NFS, area and 92% of the FS area per eye, respectively (see Table 1). The CP/FA lesion components with a greater percentage of OCT-determined subretinal lesion feature area also had greater mean (± standard deviation) thickness of the RPEDLC: 48±25 μm for GA, 61±35 μm for NGA, 83±17 μm for NFS, 151±74 μm for FS, and 33±6 μm for nonlesion areas, respectively ($P < 0.001$; see Fig. 2). In pixels designated as subretinal lesion by OCT grading, the mean RPEDLC thickness was not significant regardless of their location in areas of NGA (80±37 μm) or GA (73±22 μm, $P = 0.26$). Because so much of the NFS and FS lesion area was covered by subretinal lesion features (85% and 92%, respectively), there was little difference between the mean RPEDLC over the entire component versus in areas of OCT-determined subretinal lesion.

Among subretinal lesion features on OCT, the total component area covered by SHRM was greatest in FS (71%) and much lower in GA, NFS, and NGA (27%, 16% and 8%, respectively), whereas the area covered by PED was greater in both FS and NFS (80% and 72%, respectively) and lower in NGA and GA (32% and 18%, respectively). Although SHRM and PED features could overlap within these component areas, the relative total pixel area occupied by PED was greater than that occupied by SHRM in areas of NFS and NGA. Although the indeterminate SHRM/PED feature was present in 35% to 52% of component lesions, it extended across only 2% to 9% of any of the component areas.

Fluid was commonly identified on OCT across all 4 components (frequency range 43% to 73%). The fluid, however, covered minimal lesion component areas (2% to 6%) except in FS, for which it involved a median of 14% of the lesion area. The fluid area in FS lesions was predominantly sub-RPE fluid, which covered a median of 26% of the FS pixels per eye, in contrast to IRF and SRF, which covered a median of 4% of the FS pixels per eye. Intraretinal fluid covered a median of 13% of the NFS area,

and SRF covered a median of 9% of the NGA area. The remaining fluid involved a median of ≤3% of lesion areas.

All 68 eyes had areas with OCT features that were designated outside the CP/FA-designated TCNVL area. Analysis of these areas showed that although almost every SD-OCT feature was present within the nonlesion area, they represented <2% of the area except for the following components that were found most typically near the margin of the CP/FA-designated lesion: photoreceptor layer loss, found in 65 eyes (96%), covered a median of 7% of the nonlesion area per eye; PED, in 64 eyes (94%), covered a median of 3% of the area; and RPE atrophy with choroidal hyperreflectance and overlying material, in 58 eyes (85%), extended across a median of 3% of the area. All of the designated OCT features were absent across a median of 27% of NGA, 20% of NFS, 3% of FS, and 6% of the GA component pixels per eye, and across a median of 87% of the nonlesion pixels per eye.

From a cross-tabulation between the OCT features per overlay pixel (Table S2), we identified that subretinal lesion (SHRM, PED, or indeterminate SHRM/PED) colocalized with 68.6% of any fluid pixels: 99.5% of sub-RPE fluid pixels, 79.2% of the IRF pixels, and 56% of SRF. Distinct subretinal lesion (SHRM, PED, or indeterminate SHRM/PED) was present in 51.5% of RPE atrophy with overlying lesion. Photoreceptor loss shared 72% of pixels in eyes with RPE atrophy with overlying lesion and 94% of those with RPE atrophy without overlying lesion.

Discussion

Researchers have used OCT to compare morphologic features and to assess quantitatively retinal and subretinal lesion volumes in nAMD. The majority of analyses of OCT features have been recorded per macula or per a smaller central region of the macula (e.g., central subfield or foveal center) or have measured the largest lateral dimension of a feature.[16,17] Similarly, thickness assessments have typically used bulk measurements per macula, single measurements at the foveal center, or areas or volumes measured within different diameter circles centered on the fovea.[18-21] Some studies have evaluated colocalized fluid and PED featured in nAMD.[22] In this study, we report the first analysis of OCT features by precise macular location and extent relative to components identified on CP/FA.

After 2 years of anti-VEGF treatment for nAMD in the CATT, the distribution of 11 OCT-based features across macular areas of CP/FA-designated FS, NFS, GA, NGA, and no-lesion component reveals disparate and common retinal and subretinal morphologic features. When one considers the OCT findings across these 4 categories, there is a continuum of RPE and photoreceptor atrophy across all lesions. Retinal pigment epithelial atrophy and photoreceptor layer thinning is common not only in areas of macular atrophy, but also in areas of FS. Not surprisingly, the greatest atrophy was observed within GA areas; however, this was followed by FS, in which the median percent of RPE atrophy area per affected eye was greater than in NGA and NFS.

The difference in CP/FA appearance seemed to be affected most by the thickness and extent of the subretinal lesion complex. Fibrosis was seen on CP/FA when the subretinal lesion complex was thicker and more extensive. Although RPE atrophy with overlying lesion did not distinguish FS (median 46% of pixels in 88% of FS eyes) from GA (52% of pixels in 100% of GA eyes), RPE atrophy without lesion was almost exclusively in areas that appeared as GA on CP/FA. The difference in CP/FA appearance was influenced less by photoreceptor atrophy, which was most profound in GA (median pixel area of 85%), less in regions with FS (medial pixel area of 59%), and lower in regions with NGA and NFS (median pixel areas of 42% and 33% respectively). The extent of RPE atrophy with choroidal hypertransmission, photoreceptor loss, and degenerative change (outer retinal tubulation) in FS was striking in that it was similar to or more extensive than in NGA. Although photoreceptor loss has been documented over chronic fibrosis, the extent of RPE loss and choroidal hypertransmission has not been as clearly categorized.[1]

Subretinal lesion components were common in areas of scar, but they were also present in nearly a third or more of areas of macular atrophy. The traditional description of GA based on CP/FA intends to describe areas with loss of photoreceptors, RPE, and choriocapillaris and without subretinal tissue and fluid. During chronic multiyear anti-VEGF treatments, areas of similar-appearing sharply demarcated atrophy on CP/FA may be found within the bed of the previously active CNV complex or in dissociated areas. In the former location, these have been recognized to contain residual subretinal components reflective of prior CNV in that location.[23] In this study, although areas that appear as GA on CP/FA after 2 years of anti-VEGF treatment have loss of RPE cell pigment (resulting in choroidal hypertransmission) and photoreceptor loss, they also have retained subretinal material, though thinner than that in fibrotic scar. In the GA regions, although a median of 25% of pixels had RPE, atrophy with choroidal hypertransmission, and no overlying lesion, a median of 31% of pixels contained subretinal lesion components. The median thickness of the RPEDLC in those GA (and NGA) areas with subretinal lesion components was greater than in both GA areas without subretinal lesion components and in non-lesion areas. The thicker material here, in NGA, or even in FS may contribute to further development of atrophy as noted in a prior CATT longitudinal analysis.[7]

Atrophy of photoreceptors and RPE seems to be common across large areas of both GA and FS and beyond the clinically recognized lesion margins and less so in areas of NGA and NFS. Although areas identified as FS on CP/FA after 2 years of anti-VEGF treatment retain thicker subretinal material across the greatest lesion area, they also have loss of RPE and photoreceptors. Notably, in FS areas, choroidal hypertransmission with RPE atrophy was found in a median of 46% of FS pixels per eye, and photoreceptor layer thinning extended across a median of 59% of FS pixels per eye. Thus, although there is a distinct difference between FS and GA in the area and thickness of retained subretinal lesion material, they share high rates of photoreceptor loss (median 85% of area in GA and 59% in FS) and increased choroidal hypertransmission with loss of RPE (median 75% of area in GA and 46% in FS). Both NGA and NFS had lesser extents of photoreceptor atrophy and choroidal

hypertransmission (see Table 1). These morphologies may help to explain the poorer visual acuities found with increased duration of treatment in eyes with atrophy and FS.[7] A related finding from CATT was poorer VA with loss of the ellipsoid zone at the foveal center over areas of SHRM, though choroidal hypertransmission was not analyzed in that substudy.[24] By identifying these common retinal and subretinal anatomic elements that help to explain VA loss in both fibrosis and atrophy, we point to the potential value of OCT end points when applying therapeutics to preserve or recover RPE and photoreceptors in nAMD.

Areas designated as NGA demonstrated types and distribution of OCT features that were quite different from GA. When compared with areas of GA, areas of NGA had a smaller percentage with choroidal hypertransmission associated and RPE atrophy without overlying subretinal lesion material, an appearance that covered very tiny areas of the NGA (a median of 1% of pixels). In these eyes, the median percentage with choroidal hypertransmission associated and RPE atrophy with overlying subretinal lesion material was also lower than that observed in GA and in FS. As expected, subretinal lesions on OCT (PED, SHRM, or indeterminate SHRM/PED) were slightly more extensive in NGA than in GA, and the median RPEDLC thickness in NGA was comparable to that in GA and, again, greater than in nonlesion areas. The distinction between NGA and GA on CP/FA may also be due in part to the lesser extent of photoreceptor loss in NGA, which is about half of that in GA. The percent area of photoreceptor loss was also lower than in FS (59%). This finding helps to explain the observation that eyes with subfoveal NGA have better VA than eyes with subfoveal FS or GA but not as good as eyes without subfoveal lesions at 2 and 5 years.[25]

In CATT at 2 years, the NFS areas were flat and small lesions with well-circumscribed areas of pigmentation[1] (comprising only 2% of a central 6-mm ring area in this study). Although they had a high percentage of the area covered by lesion complex, perhaps due to their small size, they retained RPE pigmentation (only 24% of pixels with choroidal hypertransmission with RPE atrophy), had thinner RPEDLC, and had less photoreceptor layer thinning (33% of pixels). This helps to explain the retained VA documented at 2 years of treatment in eyes with subfoveal NFS in CATT.[7]

Collectively, our observations support the importance of OCT imaging to capture the full extent of retinal and residual nAMD lesion features and atrophy during treatment of nAMD, especially for clinical trials that relate morphologic features to functional outcomes. The range of morphology present within areas designated on CP/FA as GA point to the limitations in the use of that very general classification.[26] Although it is important to document the posttreatment presence or absence and the thickness of the subretinal lesion complex as this relates to the extent of photoreceptor loss, it is also important to recognize that the extent of photoreceptor loss is usually greater than the area of choroidal hypertransmission within the FS, NFS, NGA, and even GA groups. Photoreceptor loss extended across a median of 7% of nonlesion areas in 96% of eyes. Thus, photoreceptor loss alone (defined at the Classification of Atrophy Meeting as incomplete outer retinal atrophy and complete outer retinal atrophy[27]) is an important OCT variable, as this information would not be captured with designations based on choroidal hypertransmission with RPE and outer retinal atrophy.[27] This information will be especially important in studies of therapies with a goal of photoreceptor salvage or regeneration.

Our study has limitations. The significance is unclear of differences between the CP/FA component groups, which include the NFS category that had a small number of eyes (n = 7). When analyses were calculated without inclusion of NFS, there was minimal change in *P*-values, and the significance of the findings did not change. We could not consider the contribution of choroidal thickness in this analysis as it was not consistently imaged at these study visits.[3] Multimodal imaging is useful to identify polypoidal disease and components such as reticular drusen, vitelliform, and other deposits,[28] and OCT angiography has been proposed to provide delineation of risk groups in nAMD.[29-31] This study did not address infrared or OCT angiographic imaging.

Future longitudinal analyses will be important to derive information on the precursor retinal and subretinal lesion features in areas of macular atrophy, choroidal hypertransmission and RPE atrophy, and fibrosis at year 2 and their outcomes at year 5. It will be useful to perform a longitudinal study of all components of these lesions to identify the pretreatment morphology of neovascular lesions that preceded these various features and the subsequent evolution of these features several years later. This type of analysis will be especially important in light of the poorer visual outcomes in eyes with scar or atrophy and the progressive appearance of such areas after longer periods of anti-VEGF treatment for nAMD.

References

1. Daniel E, Toth CA, Grunwald JE, et al. Risk of scar in the comparison of age-related macular degeneration treatments trials. *Ophthalmology*. 2014;121:656–666.
2. Sadda SR, Tuomi LL, Ding B, et al. Macular atrophy in the HARBOR Study for neovascular age-related macular degeneration. *Ophthalmology*. 2018;125:878–886.
3. Abdelfattah NS, Al-Sheikh M, Pitetta S, et al. Macular atrophy in neovascular age-related macular degeneration with monthly versus treat-and-extend ranibizumab: findings from the TREX-AMD trial. *Ophthalmology*. 2017;124:215–223.
4. Grunwald JE, Pistilli M, Daniel E, et al. Incidence and growth of geographic atrophy during 5 years of Comparison of Age-Related Macular Degeneration Treatments Trials. *Ophthalmology*. 2017;124:97–104.
5. Grunwald JE, Daniel E, Huang J, et al. Risk of geographic atrophy in the Comparison of Age-Related Macular Degeneration Treatments Trials. *Ophthalmology*. 2014;121:150–161.
6. Jaffe GJ, Martin DF, Toth CA, et al. Macular morphology and visual acuity in the Comparison of Age-Related Macular Degeneration Treatments Trials. *Ophthalmology*. 2013;120:1860–1870.
7. Daniel E, Pan W, Ying GS, et al. Development and course of scars in the Comparison of Age-Related Macular Degeneration Treatments Trials. *Ophthalmology*. 2018;125:1034–1046.

8. Sharma S, Toth CA, Daniel E, et al. Macular, morphology and visual acuity in the second year of the Comparison of Age-Related Macular Degeneration Treatments Trials. *Ophthalmology*. 2016;123:865–875.
9. Sarwar S, Clearfield E, Soliman MK, et al. Aflibercept for neovascular age-related macular degeneration. *Cochrane Database Syst Rev*. 2016;2:CD011346.
10. Ying GS, Kim BJ, Maguire MG, et al. Sustained visual acuity loss in the comparison of age-related macular degeneration treatments trials. *JAMA Ophthalmol*. 2014;132:915–921.
11. Berg K, Roald AB, Navaratnam J, Bragadottir R. An 8-year follow-up of anti-vascular endothelial growth factor treatment with a treat-and-extend modality for neovascular age-related macular degeneration. *Acta Ophthalmol*. 2017;95:796–802.
12. Chakravarthy U, Harding SP, Rogers CA, et al. Alternative treatments to inhibit VEGF in age-related choroidal neovascularisation: 2-year findings of the IVAN randomised controlled trial. *Lancet*. 2013;382:1258–1267.
13. Toth CA, Tai V, Chiu SJ, et al. Linking OCT, angiographic, and photographic lesion components in neovascular age-related macular degeneration. *Ophthalmology Retina*. 2018;2:481–493.
14. Chiu SJ, Izatt JA, O'Connell RV, et al. Validated automatic segmentation of AMD pathology including drusen and geographic atrophy in SD-OCT images. *Invest Ophthalmol Vis Sci*. 2012;53:53–61.
15. Farsiu S, Chiu SJ, O'Connell RV, et al. Quantitative classification of eyes with and without intermediate age-related macular degeneration using optical coherence tomography. *Ophthalmology*. 2014;121:162–172.
16. Waldstein SM, Simader C, Staurenghi G, et al. Morphology and visual acuity in aflibercept and ranibizumab therapy for neovascular age-related macular degeneration in the VIEW Trials. *Ophthalmology*. 2016;123:1521–1529.
17. Wintergerst MWM, Schultz T, Birtel J, et al. Algorithms for the automated analysis of age-related macular degeneration biomarkers on optical coherence tomography: a systematic review. *Transl Vis Sci Technol*. 2017;6:10.
18. Vogl WD, Waldstein SM, Gerendas BS, et al. Analyzing and predicting visual acuity outcomes of anti-VEGF therapy by a longitudinal mixed effects model of imaging and clinical data. *Invest Ophthalmol Vis Sci*. 2017;58:4173–4181.
19. Bogunovic H, Waldstein SM, Schlegl T, et al. Prediction of Anti-VEGF treatment requirements in neovascular AMD using a machine learning approach. *Invest Ophthalmol Vis Sci*. 2017;58:3240–3248.
20. Choi CS, Zhang L, Abramoff MD, et al. Evaluating efficacy of aflibercept in refractory exudative age-related macular degeneration with OCT segmentation volumetric analysis. *Ophthalmic Surg Lasers Imaging Retina*. 2016;47:245–251.
21. Amoaku WM, Chakravarthy U, Gale R, et al. Defining response to anti-VEGF therapies in neovascular AMD. [published correction appears in *Eye (Lond)*. 2015;29:1397–1398]. *Eye (Lond)*. 2015;29:721–731.
22. Klimscha S, Waldstein SM, Schlegl T, et al. Spatial correspondence between intraretinal fluid, subretinal fluid, and pigment epithelial detachment in neovascular age-related macular degeneration. *Invest Ophthalmol Vis Sci*. 2017;58:4039–4048.
23. Holz FG, Sadda SR, Staurenghi G, et al. Imaging protocols in clinical studies in advanced age-related macular degeneration: recommendations from Classification of Atrophy Consensus Meetings. *Ophthalmology*. 2017;124:464–478.
24. Willoughby AS, Ying GS, Toth CA, et al. Subretinal hyperreflective material in the Comparison of Age-Related Macular Degeneration Treatments Trials. *Ophthalmology*. 2015;122:1846–1853.e5.
25. Comparison of Age-related Macular Degeneration Treatments Trials Research Group, Maguire MG, Martin DF, et al. Five-year outcomes with anti-vascular endothelial growth factor treatment of neovascular age-related macular degeneration: the Comparison of Age-Related Macular Degeneration Treatments Trials. *Ophthalmology*. 2016;123:1751–1761.
26. Schmitz-Valckenberg S, Sadda S, Staurenghi G, et al. Geographic atrophy: semantic considerations and literature review. *Retina*. 2016;36:2250–2264.
27. Sadda SR, Guymer R, Holz FG, et al. Consensus definition for atrophy associated with age-related macular degeneration on OCT: Classification of Atrophy Report 3. *Ophthalmology*. 2018;125:537–548.
28. Kuroda Y, Yamashiro K, Tsujikawa A, et al. Retinal pigment epithelial atrophy in neovascular age-related macular degeneration after ranibizumab treatment. *Am J Ophthalmol*. 2016;161:94–103.e1.
29. Kuehlewein L, Dustin L, Sagong M, et al. Predictors of macular atrophy detected by fundus autofluorescence in patients with neovascular age-related macular degeneration after long-term ranibizumab treatment. *Ophthalmic Surg Lasers Imaging Retina*. 2016;47:224–231.
30. Lindner M, Fang PP, Steinberg JS, et al. OCT angiography-based detection and quantification of the neovascular network in exudative AMD. *Invest Ophthalmol Vis Sci*. 2016;57:6342–6348.
31. Ichiyama Y, Sawada T, Ito Y, et al. optical coherence tomography angiography reveals blood flow in choroidal neovascular membrane in remission phase of neovascular age-related macular degeneration. *Retina*. 2017;37:724–730.

Footnotes and Financial Disclosures

Originally received: July 31, 2018.
Final revision: November 15, 2018.
Accepted: November 27, 2018.
Available online: December 3, 2018. Manuscript no. ORET_2018_321.

[1] Department of Ophthalmology, Duke University, Durham, North Carolina.

[2] Department of Biomedical Engineering, Duke University, Durham, North Carolina.

[3] Department of Ophthalmology, University of Pennsylvania, Philadelphia, Pennsylvania.

[4] Cole Eye Institute, Cleveland Clinic, Cleveland, Ohio.

*A complete listing of the clinical centers and the members of the Comparison of Age-Related Macular Degeneration Treatments Trials group is available at www.ophthalmologyretina.org.

Financial Disclosures:

The authors have made the following disclosures: C.A.T.: Grants – National Eye Institute; Personal fees (outside this work) – Alcon Laboratories; unrelated royalties; unlicensed patents on OCT analyses.

M.P.: Grants – National Institutes of Health.

S.J.C.: Patent pending on OCT analyses (segmentation and identification of layered structures in images).

E.D.: Grants – National Eye Institute.

G.J.J.: Grants – National Eye Institute, National Institutes of Health, Department of Health and Human Services; Personal fees (outside this work) – Heidelberg Engineering (consultant), Novartis (consultant), Regeneron (consultant).

G.Y.: Personal fees – Chengdu Kanghong Biotechnology Co. Ltd, Code C (biostatistical consultant) and Ziemer Ophthalmic Systems AG (biostatistical consultant) outside this work.

S.F. — Grants from the National Eye Institute, National Institutes of Health, and Department of Human Services, unlicensed patents on OCT analyses.

M.G.M.: Grants – National Eye Institute outside this work, personal fees from Genentech/Roche (Data and Safety Monitoring Committee).

Supported by cooperative agreements U10 EY017823, U10 EY017825, U10 EY017826, U10 EY017828, and U10 EY023530 from the National Eye Institute, National Institutes of Health, and the Department of Health and Human Services, Bethesda, Maryland. The funding organization participated in the design and conduct of the study and review of the article. ClinicalTrials.gov number NCT00593450.

HUMAN SUBJECTS: Human subjects were included in this study. The study was approved by an institutional review board associated with each center and was compliant with the Health Insurance Portability and Accountability Act regulations. The study was performed in accordance with the tenets of the Declaration of Helsinki. All participants provided written informed consent.

No animal subjects were used in this study.

Author contributions:

Research design: Toth, Pistilli, Daniel, Grunwald, Jaffe, Martin, Farsui, Maguire

Data collection: Toth, Tai, Pistilli, Daniel, Grunwald, Maguire

Data analysis and interpretation: Toth, Tai, Pistilli, Chiu, Winter, Daniel, Grunwald, Ying, Maguire

Obtained funding: Martin, Maguire, Jaffe

Manuscript preparation: Toth, Tai, Pistilli, Chiu, Winter, Daniel, Grunwald, Jaffe, Martin, Ying, Farsiu, Maguire

Abbreviations and acronyms:
AMD = age-related macular degeneration; **CATT** = Comparison of Age-Related Macular Degeneration Treatments Trials; **CNV** = choroidal neovascularization; **CP** = color photograph; **FA** = fluorescein angiography; **FS** = fibrotic scar; **GA** = geographic atrophy; **IRF** = intraretinal fluid; **nAMD** = neovascular AMD; **NFS** = nonfibrotic scar; **NGA** = nongeographic atrophy; **OCT** = optical coherence tomography; **NSR** = neurosensory retina; **PED** = pigment epithelial detachment; **ORT** = outer retinal tubulation; **RPE** = retinal pigment epithelium; **RPEDLC** = RPE + drusen + lesion complex; **SD-OCT** = spectral domain-OCT; **SHRM** = subretinal highly reflective material; **SRF** = subretinal fluid; **TCNVL** = total CNV lesion; **TD** = time domain; **VA** = visual acuity; **VEGF** = vascular endothelial growth factor.

Correspondence:
Cynthia A. Toth, Department of Ophthalmology, Duke University Medical Center, 2351 Erwin Road, Box 3802, Durham, NC 27710. E-mail: cynthia.toth@duke.edu.

Pictures & Perspectives

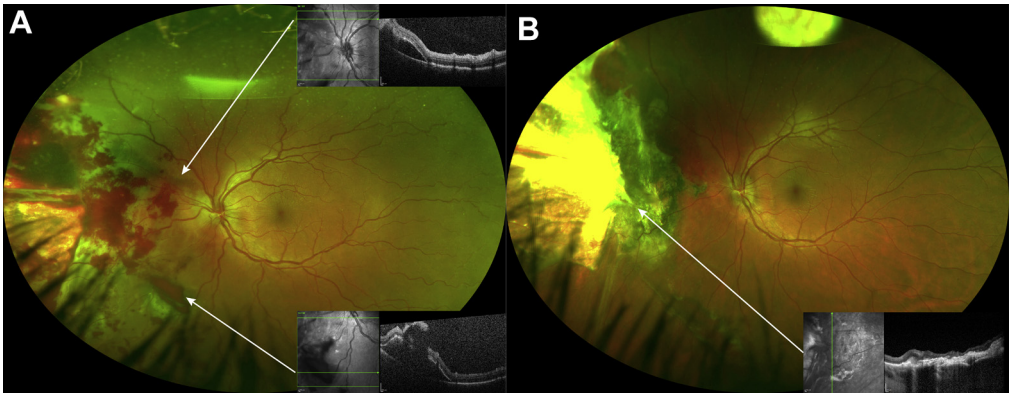

Sclopetaria and Spontaneous Resolution of Subretinal Fluid

Fundus imaging (**A**) of a 16-year-old boy with traumatic chorioretinal rupture (chorioretinitis sclopetaria) 1 day after a high-velocity paintball pellet injury. There was mild macular commotio retinae, preretinal, intraretinal, and subretinal hemorrhage, and full-thickness disruption of the nasal retina and choroid with retracted, rolled edges with visible bare sclera. OCT confirmed subretinal fluid (SRF) in the superior and inferior midperiphery (**A**, insets). Two months later, without any intervention, there was complete spontaneous resolution of SRF, development of chorioretinal atrophy and fibrosis (**B**), and resolution of macular commotio retinae. Visual acuity improved from 20/100 to 20/20.

Mark Goerlitz-Jessen, MD
Mohsin H. Ali, MD
Dilraj S. Grewal, MD

Department of Ophthalmology, Duke University, Duke Eye Center, Durham, North Carolina